ELSEVIER

Journal of Alloys and Compounds 451 (2008) 521–525

Journal of ALLOYS AND COMPOUNDS

www.elsevier.com/locate/jallcom

Some recent results on the correlation of nano-structural and redox properties in ceria-zirconia mixed oxides

S. Bernal*, G. Blanco, J.J. Calvino, J.C. Hernández,
J.A. Pérez-Omil, J.M. Pintado, M.P. Yeste

Departamento de Ciencia de los Materiales, Ingeniería Metalúrgica y Química Inorgánica, Facultad de Ciencias,
Universidad de Cádiz, Campus Río San Pedro, E-11510 Puerto Real (Cádiz), Spain

Abstract

Some recent results on the redox behaviour of thermally aged ceria-zirconia mixed oxides with Ce/Zr molar ratios typically ranging from 50/50 to 70/30 are briefly reviewed. In accordance with them, a tentative model allowing us to correlate ageing conditions, surface and bulk nano-structural properties of the oxides, and changes occurred in their redox behaviour is proposed.

As revealed by the analysis of appropriate chemical studies and the nano-structural information provided with High Resolution Transmission (HREM) and High Angle Annular Dark Field-Scanning Transmission (HAADF-STEM) electron microscopies, the presence/absence of a pyrochlore-related κ-phase in the aged oxides plays a key role in determining their redox response. In the low-temperature region ($T_{red} \leq 773$ K), the enhanced reducibility exhibited by the oxide resulting from a high-temperature reduction/mild re-oxidation ageing cycle (SR-MO sample) is interpreted as due to kinetic reasons, the occurrence of the κ-like phase in its surface being responsible for a faster H_2 chemisorption, the rate controlling step of the overall reduction process. By contrast, in the high-temperature range ($T_{red} \geq 973$ K), the observed differences of reducibility would have a thermodynamic origin, which may be correlated with the total amount of κ-like phase present in the aged sample.

Keywords: Ceria-zirconia; Nano-structure; κ-like phase; Redox behaviour

1. Introduction

Compared to cerium dioxide, ceria-zirconia mixed oxides are generally acknowledged to show enhanced textural [1–3] and redox properties [1,4–6]. Consequently to this, the interest on their catalytic applications has rapidly grown during the last decade [7–12]. An important part of the research effort has been devoted to the investigation of their oxygen exchange properties. Particularly noticeable are the reversible changes of reducibility induced on the ceria-zirconia samples by appropriate modification of the thermal ageing conditions [13–15]. Because of the very challenging nature of this phenomenon, numerous studies have dealt with this topic in recent years [16–28].

This work is aimed at briefly reviewing the latest investigations on the origin of the reversible changes of reducibility observed in thermally aged ceria-zirconia mixed oxides. As deduced from the analysis of the results presented here, significant progress has been made in the understanding of some fundamental aspects of this phenomenon. In accordance with this, a model allowing to rationalise the relationship existing between thermal ageing conditions, nano-structural properties and redox behaviour of ceria-zirconia mixed oxides is proposed.

2. Results and discussion

2.1. Earliest evidence of reversible changes of reducibility in thermally aged ceria-zirconia mixed oxides

The very first experimental evidences of reversible changes in the reducibility of thermally aged ceria-zirconia mixed oxides with Ce/Zr molar ratios typically ranging from 50/50 to 70/30 were reported in the latest 1990's [13–15]. By using, respectively, a solid electrolyte potentiostatic technique [13,14] and a conventional temperature-programmed reduction-mass spectrometry (TPR-MS) device [15] to monitor the redox state of

---

* Corresponding author.
E-mail address: serafin.bernal@uca.es (S. Bernal).

0925-8388/$ – see front matter © 2007 Elsevier B.V. All rights reserved.
doi:10.1016/j.jallcom.2007.04.201

the investigated samples, these earliest studies clearly showed that, upon alternating redox ageing cycles consisting of severe reduction treatment (SR; $T_{red} > 1173$ K), followed by either a mild (MO, $T_{oxn} \leq 873$ K) or severe (SO, $T_{oxn} \geq 1173$ K) re-oxidation step, dramatic changes in the redox response of the resulting oxides could be reversibly induced. Specifically, the SR-MO ageing cycles lead to mixed oxides with enhanced low-temperature reducibility, whereas the SR-SO ones induce the opposite effect, i.e. a loss of redox activity. Later on, several other authors have reported quite similar findings [16–18,26,27]. Most of these studies have been carried out on oxide samples with Ce/Zr molar ratios typically ranging from 50/50 to 70/30, those with Ce/Zr = 50/50 having received a very special attention [14,16–18,24]. Accordingly, the phenomenon should be nowadays considered as a well established characteristic feature of the redox chemistry of ceria-zirconia mixed oxides with intermediate Ce/Zr molar ratios.

2.2. Structural studies on thermally aged ceria-zirconia mixed oxides

The likely existence of a close relationship between the chemical effects briefly summarised in Section 2.1 and the structural nature of the thermally aged ceria-zirconia samples was soon recognized. Accordingly, a considerable research effort has been devoted to gain a deeper understanding of the structural changes induced on the oxides by the ageing cycles mentioned above. A number of techniques, including X-ray diffraction (XRD) [13,14,18,20,23,24,31], EXAFS [29,30,31], Raman spectroscopy [14,17,18,24], High Resolution Electron Microscopy (HREM) [21,22,25,26] and High Angle Annular Dark Field Scanning-Transmission Electron Microscopy (HAADF-STEM) [25] have been applied in these structural investigations. Among them, XRD, Raman spectroscopy, and more recently HREM and HAADF-STEM have been the most extensively applied ones.

As a consequence of the acknowledged structural complexity of ceria-zirconia mixed oxide systems with intermediate chemical compositions, a variety of phases has been reported to occur in the thermally aged samples; among them those referred to as t, t′, t″, t* and κ, have often been considered in the literature [13,14,18,24–26]. Despite the difficulty inherently associated to the eventual occurrence of such a large variety of phases, there are some structural facts which may be considered as well established. As outlined by a number of authors [13,18,20,23,26] order ↔ disorder phenomena induced on the Ce–Zr cationic sub-lattice by the SR-MO and SR-SO ageing treatments would play an essential role in determining their redox response. In effect, it is generally acknowledged that associated to SR-type reduction treatments an oxygen deficient, cation-ordered, pyrochlore-type phase, is formed. If this reduced phase is further re-oxidised under mild conditions (MO), the cationic sub-lattice remains unmodified and a highly active oxidized pyrochlore (κ-like phase) is formed. The occurrence of Ce–Zr ordering in the κ-like phase is experimentally evidenced by the appearance of characteristic super-structure features in the XRD diagrams [18,20,23], as well as in the HREM [25,26] and HAADF-STEM [25] images of this phase. Fig. 1A–C report on the HAADF-STEM study supporting this statement.

On the contrary, a severe re-oxidation treatment (SO) would destroy the ordered cationic structure, thus leading to an oxide sample with a random distribution in its Ce–Zr sub-lattice. Fig. 1D and E show, respectively, HREM images corresponding to SR-MO and SR-SO mixed oxide samples. In good agreement with the proposal above, the image contrasts and digital diffraction patterns (DDP) for the SR-MO sample, Fig. 1D, show the occurrence of the superstructure features characterising the ordered phase. These features can hardly be observed in the case SR-SO sample, Fig. 1E. Also noticeable in Fig. 1D and E is the remarkable difference of morphology exhibited by the SR-MO and SR-SO aged oxides [26].

2.3. Recent results on the relationship existing between nano-structural properties and redox behaviour of ceria-zirconia mixed oxides

In recent years several authors [13–18,20,24,26] have investigated the relationship existing between structural properties and reversible changes of reducibility observed in ceria-zirconia samples submitted to successive ageing cycles in which SR-MO and SR-SO routines were alternatively applied. As a result significant progress has been made in the understanding of this very challenging phenomenon. Thus, in ref. [26], a systematic nano-structural and chemical characterisation study of two thermally aged (SR-MO and SR-SO) $Ce_{0.62}Zr_{0.38}O_2$ samples is reported. In addition to HREM imaging, temperature programmed reduction-mass spectrometry (TPR-MS), H_2 volumetric chemisorption and oxygen storage capacity (OSC) measurements were performed.

Fig. 2 shows the traces recorded for H_2 (m/e = 2) and H_2O (m/e = 18) in the corresponding TPR-MS experiments. As expected, the reducibility of the SR-MO sample is significantly better. Also remarkable, no delay in the H_2O formation as compared to the H_2 consumption can be observed. This constitutes a first indication of the role of hydrogen adsorption in the control of the overall low-temperature redox response of the samples. To confirm this hypothesis, two additional studies were performed [26]. Firstly, the hydrogen chemisorption on both SR-MO and SR-SO samples was investigated. As discussed in ref. [26], a clear correlation could be established between low-temperature reducibility of the oxides, as revealed by TPR-MS, Fig. 2, and their capability to activate the H_2 molecule, much larger in the case of SR-MO sample. This conclusion is further supported by the dramatic enhancement of the low-temperature reducibility of both SR-MO and SR-SO samples upon dispersing a small amount of rhodium on their surface [26]. As exemplified in bottom part of Fig. 3 by the TPR-MS study carried out on a 0.3%Rh/SR-SO sample, in the presence of Rh, an alternative, more efficient, mechanism of hydrogen activation leading to atomic hydrogen chemisorbed on the support, the spillover, appears. Consequently to this, a drastic shift towards lower temperatures is observed in the main peak of the corresponding TPR-MS diagrams.

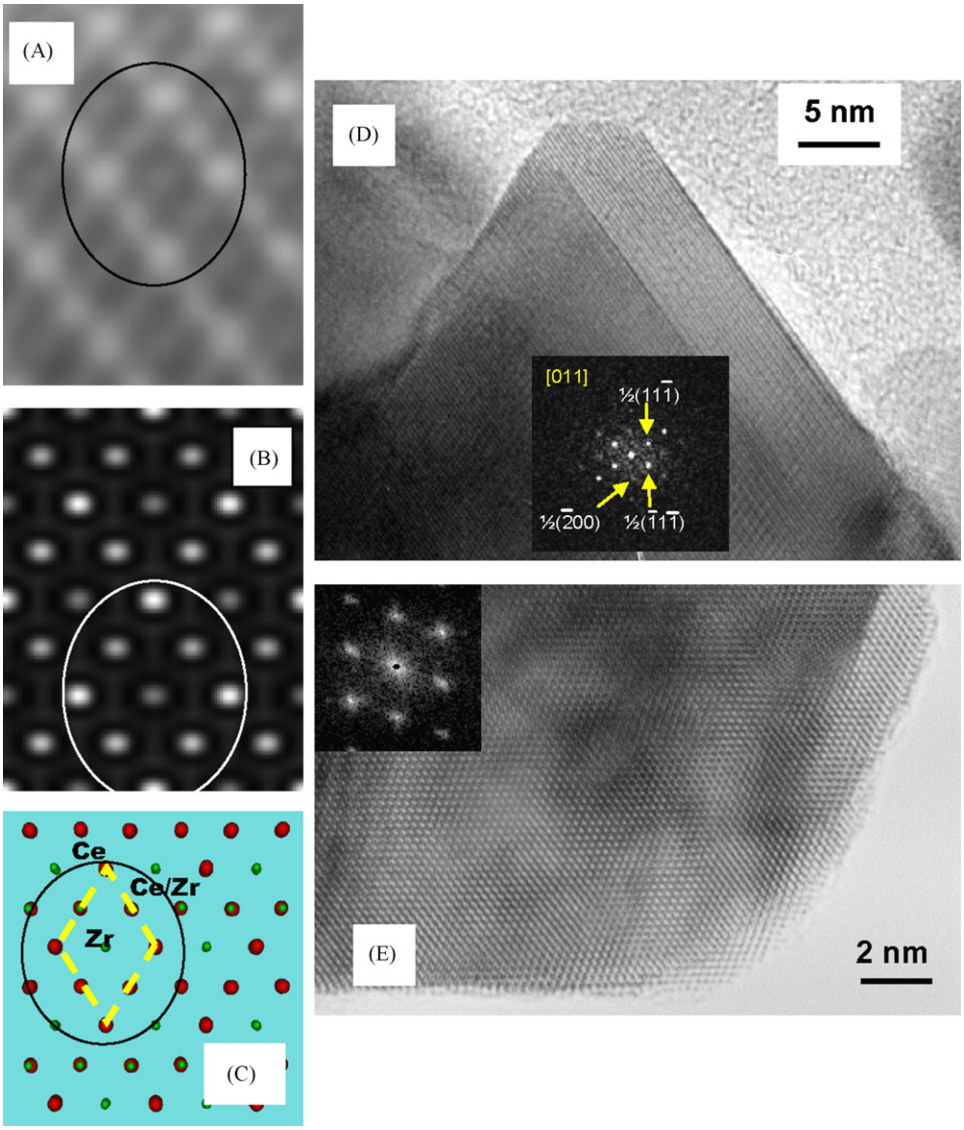

Fig. 1. Electron microscopy studies on thermally aged ceria-zirconia mixed oxides. HAADF-STEM of a $Ce_{0.68}Zr_{.32}O_2$ SR-MO sample [25]. Experimental image (A). Computer simulated image (B) and structural model (C) of pyrochlore-type ordered cationic sub-lattice used as input in the image calculations. Projections along the [1 1 0] direction. Differences of contrast intensity in both the experimental (A) and simulated (B) images are interpreted as due to the occurrence of three types of cationic columns containing, respectively: Ce, Ce + Zr and Zr (Ce–Zr ordering). HREM images showing the remarkable structural and morphological differences existing between the $Ce_{0.62}Zr_{0.38}O_2$ SR-MO (D) and SR_0SO (E) samples [26]. The characteristic super-structure features of the κ-like phase can only be observed in the image and DDP recorded for SR-MO sample (D).

The oxygen storage capacity data do also provide with some very relevant pieces of information, Fig. 3. From the analysis of data reported in this figure, a number of interesting conclusions can be drawn.

As deduced from Fig. 3A, for the bare oxides, throughout the whole range of investigated reduction temperatures, the SR-MO sample always shows higher OSC values than the SR-SO one.

In the presence of Rh, Fig. 3B, a very significant increase of the low-temperature OSC values is observed on both SR-MO and SR-SO samples. This suggests that, in the low-temperature domain, for the bare oxides, the OSC values do not account for true equilibrium reduction states, i.e. they are mainly determined by kinetic factors associated with their respective capabilities for activating the H_2 molecule. As suggested by both the TPR-MS diagrams, Fig. 2, and the OSC values, Fig. 3B, the presence of Rh would remove this kinetic restriction, thus allowing that OSC values much closer to the thermodynamic limit are obtained. If so, even at the lowest reduction temperature, 473 K, surface creation of oxygen vacancies or its diffusion into the bulk of the oxide should not represent kinetic limitations to the overall reduction process. By contrast, the high-temperature OSC values for the bare oxides and the supported Rh samples are much closer, thus suggesting that, in this domain of reduction temperatures, the recorded OSC values are mainly determined by thermodynamic factors.

Regarding the origin of the differences of redox behaviour found in the bare oxide samples, a clear distinction should therefore be made between high- and low-temperature domains. In

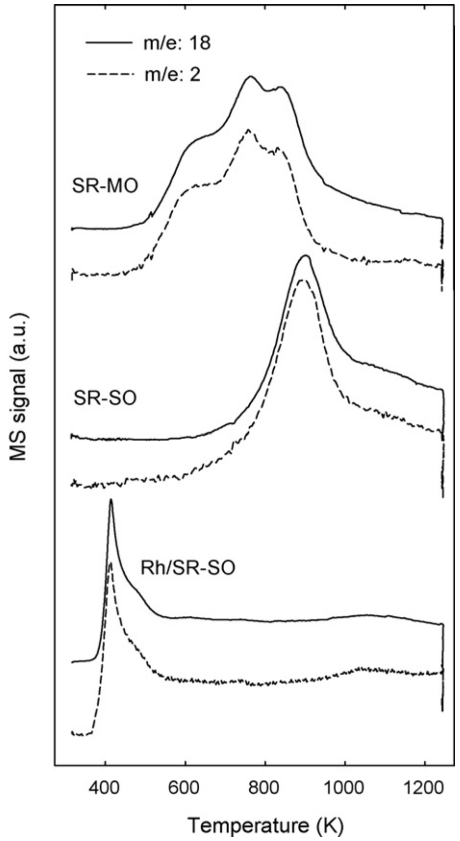

Fig. 2. TPR-MS traces for H_2 (m/e = 2) and H_2O (m/e = 18) corresponding to a $Ce_{0.62}Zr_{0.38}O_2$ sample submitted, respectively, to SR-MO and SR-SO ageing routines. To facilitate the comparison between H_2 and H_2O traces, hydrogen consumption is plotted as a positive signal. The effect of supported Rh on the reducibility of the oxides is exemplified by the diagrams recorded for the 0.3%Rh/SR-SO sample, bottom part of the figure.

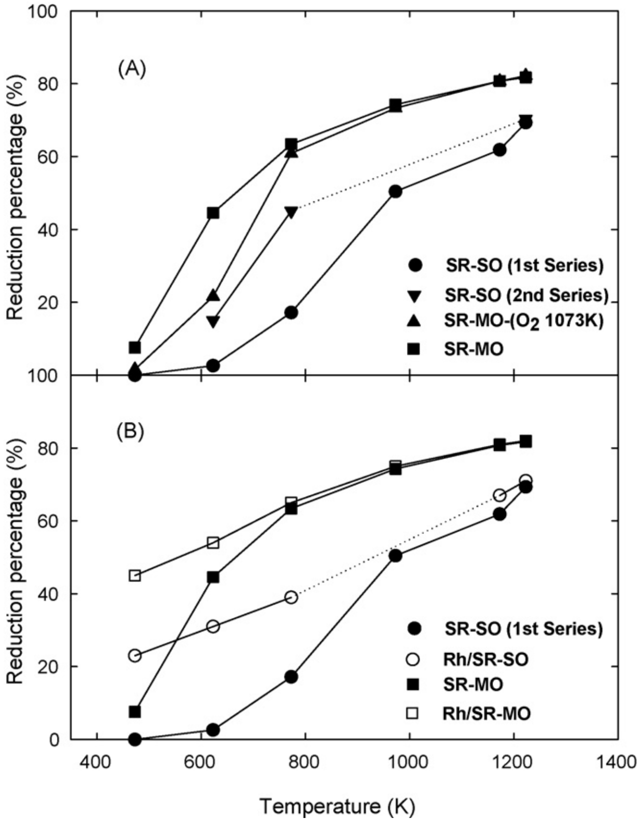

Fig. 3. Ultimate OSC data corresponding to a $Ce_{0.62}Zr_{0.38}O_2$ sample submitted, respectively, to SR-MO and SR-SO ageing routines. Bare oxides (Part A); influence of highly dispersed Rh (Part B). OSC values were determined by O_2 chemisorption at 473 K of samples reduced for 1 h, in a flow of 5%H_2/Ar, at the indicated temperatures. See ref. [26] for further experimental details.

the low-temperature region, the differences of reducibility would be determined by kinetic factors, whereas at the highest reduction temperatures they would reflect the intrinsic thermodynamic differences existing between SR-MO and SR-SO samples. We should conclude, accordingly, that order ↔ disorder phase transitions induced by the SR-MO and SR-SO ageing routines have a double effect. First, they strongly modify the surface properties of the resulting oxides, thus affecting their capability for H_2 activation, and therefore their low-temperature redox response, much better in the case of the SR-MO sample. Second, the ageing protocol does also modify the bulk structural properties of the oxides, and consequently, their thermodynamic properties. As very recently discussed in ref. [32], entropy factors play a key role in determining the thermodynamic stability of the different aged phases.

In good agreement with some earlier studies [24], the results reported here show that, from a thermodynamic point of view, the reducibility of the SR-MO, the one mainly consisting of an ordered phase, is higher than that of the SR-SO sample, the one exhibiting a random distribution in the Ce–Zr cationic sublattice.

Fig. 3A includes some additional interesting OSC data. They correspond, respectively, to the SR-MO sample further treated with 5%O_2/He, for 30 min at 1073 K and to the SR-SO sample resulting from a first series of OSC measurements, i.e. further reduced for 1 h at 1223 K in a flow of 5%H_2/Ar, and finally re-oxidised at 473 K. The behaviour of these two additional samples is fully consistent with the model suggested in the previous paragraphs. In effect, compared to the SR-MO and SR-SO oxides, from which they were obtained, these samples show significantly different low-temperature OSC data, i.e. those determined by the surface properties of the oxides. By contrast, the high-temperature OSC values, i.e. those determined by their thermodynamic bulk properties, are much closer. We should conclude, accordingly, that the additional treatments applied, respectively, to the SR-MO and SR-SO samples essentially modify their surface properties without significant modification of their bulk structure. In the case of the SR-MO sample, the additional short oxidation treatment at 1073 K, would thus produce a surface-modification of the κ-like phase, with inherent loss of its hydrogen activation capability. In the case of the SR-SO one, on the contrary, the additional reduction treatment at 1223 K, followed by a mild re-oxidation at 473 K, might well induce a surface regeneration of the ordered phase, mainly affecting the capability of the sample for activating the H_2 molecule, with inherent enhancement of the low-temperature reducibility [26].

Acknowledgements

This work has been supported by MEC/FEDER-EU (Project: MAT 2005-00333) and the *Junta de Andalucía* (FQM-110 and FQM-334).

References

[1] M. Pijolat, M. Prin, M. Soustelle, O. Touret, P. Nortier, J. Chem. Soc. Faraday Trans. 91 (1995) 3941.

[2] G. Colón, F. Valdivielso, M. Pijolat, R.T. Baker, J.J. Calvino, S. Bernal, Catal. Today 50 (1999) 271.

[3] J. Kaspar, P. Fornasiero, M. Graziani, Catal. Today 50 (1999) 285.

[4] P. Fornasiero, R. Di Monte, G. Ranga Rao, J. Kaspar, S. Meriani, A. Trovarelli, J. Catal. 151 (1995) 168.

[5] R. Di Monte, J. Kaspar, J. Mater. Chem. 15 (2005) 633.

[6] D. Duprez, C. Descorme, in: A. Trovarelli (Ed.), Catalysis by Ceria and Related Materials, Imperial College Press, London, 2002, pp. 243–280 (chapter 7).

[7] E. Aneggi, M. Boaro, C. Leitemburg, G. Dolcetti, A. Trovarelli, J. Alloys Compd. 408–412 (2006) 1096.

[8] J.C. Serrano-Ruiz, J. Luettich, A. Sepúlveda-Escribano, F. Rodríguez-Reinoso, J. Catal. 241 (2006) 45.

[9] H. Oguchi, T. Nishiguchi, T. Matsumoto, H. Kanai, K. Utani, Y. Matsumura, S. Steam, Appl. Catal. A: Gen. 281 (2005) 69.

[10] J.C. Vargas, S. Libs, A.C. Roger, A. Kiennemann, Catal. Today 107–108 (2005) 417.

[11] K. Kusakabe, K. Sotowa, T. Eda, Y. Iwamoto, Fuel Process. Technol. 86 (2004) 319.

[12] A. Wootsch, C. Descorme, D. Duprez, J. Catal. 225 (2004) 259.

[13] N. Izu, T. Omata, S. Otsuka-Yao-Matsuo, J. Alloys Compd. 270 (1998) 107.

[14] S. Otsuka-Yao-Matsuo, T. Omata, N. Izu, H. Kishimoto, J. Solid State Chem. 138 (1998) 47.

[15] R.T. Baker, S. Bernal, G. Blanco, A. Cordon, J.M. Pintado, J.M. Rodriguez-Izquierdo, F. Fally, V. Perrichon, Chem. Commun. (1999) 149.

[16] P. Fornasiero, T. Montini, M. Graziani, J. Kaspar, A.B. Hungría, A. Martínez-Arias, J.C. Conesa, Phys. Chem. Chem. Phys. 4 (2002) 149.

[17] T. Montini, M.A. Bañares, N. Hickey, R. Di Monte, P. Fornasiero, J. Kaspar, M. Graziani, Phys. Chem. Chem. Phys. 6 (2004) 1.

[18] T. Montini, N. Hickey, P. Fornasiero, M. Graziani, M.A. Bañares, M.V. Martínez-Huerta, I. Alessandri, L.E. Depero, Chem. Mater. 17 (2005) 1157.

[19] R. Di Monte, J. Kaspar, Topics Catal. 28 (2004) 47.

[20] A. Suda, Y. Ukyo, K. Yamamura, H. Sobukawa, T. Sasaki, Y. Nagai, T. Tanabe, M. Sugiura, J. Ceram. Soc. Jpn. 112 (2004) 586.

[21] T. Sasaki, Y. Ukyo, K. Kuroda, S. Arai, H. Saka, J. Electron. Microsc. 52 (2003) 309.

[22] T. Sasaki, Y. Ukyo, A. Suda, M. Sugiura, K. Kuroda, S. Arai, H. Saka, J. Ceram. Soc. Jpn. 111 (2003) 382.

[23] H. Kishimoto, T. Omata, S. Otsuka-Yao-Matsuo, K. Ueda, H. Hosono, H. Kawazoe, J. Alloys Compd. 312 (2000) 94.

[24] N. Izu, H. Kishimoto, T. Omata, K. Ono, S. Otsuka-Yao-Matsuo, Sci. Technol. Adv. Mater. 2 (2001) 397.

[25] J.A. Pérez Omil, S. Bernal, J.J. Calvino, J.C. Hernández, C. Mira, M.P. Rodríguez-Luque, R. Erni, N.D. Browning, Chem. Mater. 17 (2005) 4282–4285.

[26] M.P. Yeste, J.C. Hernández, S. Bernal, G. Blanco, J.J. Calvino, J.A. Pérez Omil, J.M. Pintado, Chem. Mater. 18 (2006) 2750.

[27] S. Bernal, G. Blanco, J.J. Calvino, J.M. Gatica, J.A. Pérez Omil, J.M. Pintado, Topics Catal. 28 (2004) 31.

[28] S. Otsuka-Yao-Matsuo, N. Izu, T. Omata, K. Ikeda, J. Electrochem. Soc. 145 (1998) 1406.

[29] Y. Nagai, T. Yamamoto, T. Tanaka, S. Yoshida, T. Nonaka, T. Okamoto, A. Suda, M. Sugiura, Catal. Today 74 (2002) 225.

[30] S. Lemaux, A. Bensaddik, A.M.J. van der Eerden, H. Bitter, D.C. Koningsberger, J. Phys. Chem. B 105 (2001) 4810.

[31] J.A. Rodríguez, J.C. Hanson, J.Y. Kim, G. Liu, A. Iglesias, M. Fernández García, J. Phys. Chem. B 107 (2003) 3535.

[32] P.R. Shah, T. Kim, G. Zhou, P. Fornasiero, R.J. Gorte, Chem. Mater. 18 (2006) 5363.